Springer

KSME

Journal of Mechanical Science and Technology 29 (2) (2015) 769~776
www.springerlink.com/content/1738-494x
DOI 10.1007/s12206-015-0138-6

Parameter design and analysis in continuous drive friction welding of Al6061/SiCp composites †

R. Adalarasan[1,*] and A. Shanmuga Sundaram[2]

[1]*Department of Mechanical Engineering, Saveetha Engineering College, Chennai-602105, India*
[2]*Department of Mechanical Engineering, Sree Sastha Institute of Engineering and Technology, Chennai-600123, India*

(Manuscript Received May 28, 2014; Revised October 3, 2014; Accepted November 7, 2014)

Abstract

Continuous drive friction welding (FW) had found profound industrial applications as an economical solid state joining process. The welding parameters such as frictional pressure, upset pressure, burn off length and rotational speed were found to influence the quality of joints. In the present study, Al6061/SiC_p rods were joined by friction welding. The welding trials were designed by using Taguchi's L_9 orthogonal array. Tensile strength and micro hardness of the joints were observed as the quality characteristics after each trial. The urge for parameter design had prompted the disclosure of a new integrated methodology based on technique for order of preference by similarity to ideal solution (TOPSIS) and grey relational analysis (GRA). The effectiveness of the proposed approach of T-GRA was validated by conducting a confirmation test and the field emission scanning electron microscope (FESEM) images of the fractured surface were also examined.

Keywords: Continuous drive friction welding; Composites; TOPSIS; Grey relational analysis; Optimization

1. Introduction

The aluminium based metal matrix composites (MMCs) were found to possess good mechanical properties like strength, stiffness and resistance to wear [1]. Both metallurgical and microstructural defects were observed during conventional joining of aluminium alloys by fusion welding techniques [2]. Hence a solid state joining process like friction welding (FW) could offer a feasible solution for joining MMCs. The temperature generated during the process of friction welding was kept well below the recrystallization temperature hence eliminating unnecessary metallurgical changes in the parent material. The bond was produced by mechanical rubbing action of one part against the other to produce required thermal flux. An axial pressure was applied to ensure plastic flow of material around the interface to form the bond with lesser energy input and reduced heat affected zone (HAZ) [3]. FW was employed effectively to join AISI 1040 alloy rods of different diameter for varying applications and the joints were found to possess good mechanical properties [4]. The welding parameters like frictional pressure (FP), upset pressure (UP), burn off length (BOL) and rotational speed (S) were observed to affect the quality characteristics of the joints [5]. The frictional pressure and speed were found to influence the thermal flux developed during welding and upset pressure was observed to be significant in affecting the plastic flow of material around the interface [6, 7]. Rotational speed and upset pressure were found to influence the quality of joints formed with MMCs [8]. However finding an optimal welding condition for good bond characteristics requires a considerable number of trials with the weld input parameters chosen based on the operator's skill [9]. The methods used for solving multi response optimization problems include grey relational analysis (GRA), principal component analysis (PCA), data envelopment analysis and meta-heuristic methods [10].

An artificial intelligence approach using artificial neural network (ANN) and genetic algorithm (GA) was used for modelling the quality characteristics effectively and the results were validated [11]. However GA does not scale well with complexity and requires a good setting of its own parameters. Training the back propagation neural network was also observed to be difficult and tedious. The response surface methodology (RSM) along with central composite design could be used to design the experiments and obtain optimal results [12]. RSM was employed successfully to optimize the parameters in resistance welding but the technique was observed to lose its power in irregular regions [13]. A hybrid approach of optimization using GRA and PCA was found to take the merits

*Corresponding author. Tel.: +91 9444108703, Fax.: +91 442 681 1009
E-mail address: adalno1@yahoo.co.in
† Recommended by Associate Editor Young Whan Park

of techniques adopted and could predict optimal solution [14]. GRA was observed to be effective in optimizing the process parameters and analysis of variance (ANOVA) was used to find the contribution of various parameters [15]. Technique for order of preference by similarity to ideal solution (TOPSIS) was an intuitive and easy to implement ranking method. It was a multi-criteria decision making (MCDM) technique applied to solve problems with a finite number of options [16]. TOPSIS was used for ranking the responses with respect to several criteria parameters and was found to be useful in multi response optimization [17, 18].

From the review of literature, it was observed that parameter design in friction welding of Al6061/SiCp composites using an integrated methodology was scarce. Hence a new integrated algorithm involving TOPSIS and grey relational analysis (T-GRA) was presented for multi response optimization.

2. Experimental design and observations

2.1 Materials

The Al6061 aluminium alloy was reinforced (20% weight fraction) with fine particles of silicon carbide (SiC). The MMC was prepared by dispersing the reinforcing particles in liquid Al6061 using the process of double stage stir casting. The cast Al6061/SiCp rods of diameter 17 mm and length 75 mm were subjected to radiographic inspection to identify the defective pieces and discard them. Finally the selected rods were turned to a diameter of 14 mm and faced at their ends to reduce the length to 70 mm. The stir casting setup employing an INDFURR electric furnace rated at 4.5 KW and operating on a 230 V single phase alternating current is shown in Fig. 1(a). The stirred slurry was poured into a pre-heated mould to cast Al6061/SiCp rods as shown in Fig. 1(b). The field emission scanning electron microscope (FESEM) image displaying the uniform distribution of the SiC particles in Al6061 matrix is shown in Fig. 1(c).

(a)

(b)

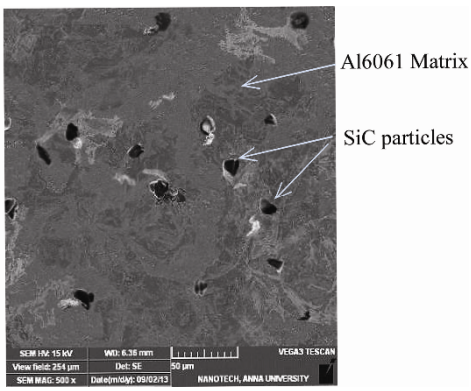

(c)

Fig. 1. (a) Stir casting setup; (b) cast Al6061/SiCp rod; (c) FESEM image showing the SiC particles in aluminium matrix.

2.2 Experimental setup

In continuous drive friction welding, an AC motor was used to drive the spindle to which one part to be joined was attached and rotated. The other part was held in a system capable of imparting axial motion to bring them together and form the joint. A servo valve controlled load cell was used to read the frictional and upset forces while a PLA based system was employed to ensure the transition from friction phase to forging phase automatically. The experimental setup is shown in Fig. 2.

The schematic diagram of continuous drive friction welding is shown in Fig. 3. One part to be joined was attached to the rotating chuck while the other was held in a sliding arrangement capable of applying axial pressure. When the two parts touch each other frictional heat was generated to produce thermal softening at the interface and an axial pressure was applied to allow plastic flow of material and form the bond.

The dominant friction welding parameters included in the study were frictional pressure (FP), upset pressure (UP), burn off length (BOL) and rotational speed (S) [4-8]. A sufficient number of trial experiments were carried out to identify the range of process parameters for forming joints without any visible defects. The parameters were varied at three levels as per Taguchi's L_9 orthogonal array and two replicates were formed. Equal overhung length was ensured on both parts to be joined during various trials. The welding trials were conducted at random to avoid the extraneous effects [10]. The responses observed were tensile strength (TS), micro hardness in the weld area (WA_H) and at the heat affected zone (HAZ_H). A Vickers hardness tester was used to find the micro hardness value by applying a load of 500 gm for 20 seconds and the sample for tension test was prepared according to ASTM B557 standard. The joints were characterized by the presence

(a)

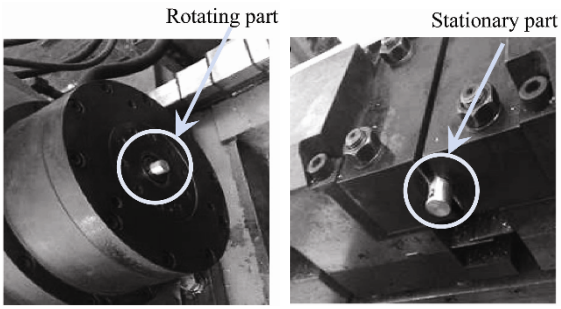

(b) (c)

Fig. 2. (a) Friction welding machine; (b) part held in chuck; (b) stationary part.

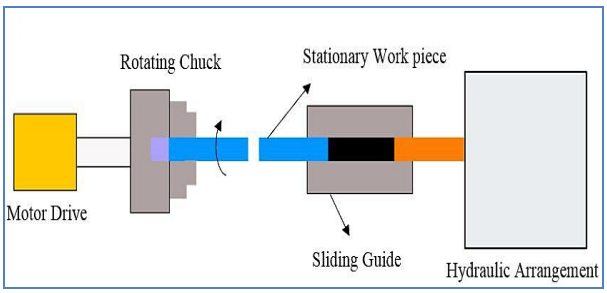

Fig. 3. Schematic diagram of continuous drive friction welding process.

of reduced HAZ compared to those formed with fusion welding techniques. The friction welded area subjected to the effects of severe plastic deformation was almost restricted to the bond line. The HAZ was observed to spread to a maximum distance of 2 mm on both sides of bond line [8]. The micro hardness in weld area was higher than that observed in the HAZ. The macro-view of joints is shown in Fig. 4 and the responses observed for various trials are listed in Table 1.

3. Integrated methodology of technique for order of preference by similarity to ideal solution (TOPSIS) and grey relational analysis (T-GRA)

This integrated algorithm of T-GRA employed for parameter design in friction welding was described in Sec. 3.1 (Phase I: TOPSIS) and Sec. 3.2 (Phase II: Grey Relational Analysis).

Table 1. Responses observed for various trials.

Trial	FP (MPa)	UP (MPa)	S (rpm)	BOL (mm)	Responses		
					TS (N/mm^2)	WA_H	HAZ_H
1	45	50	1000	1	93.98	73	69
2	45	75	1500	2	90.70	79	76
3	45	100	2000	3	92.61	67	62
4	55	50	1500	3	88.21	80	77
5	55	75	2000	1	83.47	74	70
6	55	100	1000	2	81.65	95	89
7	60	50	2000	2	90.30	85	83
8	60	75	1000	3	116.58	61	59
9	60	100	1500	1	83.57	95	91

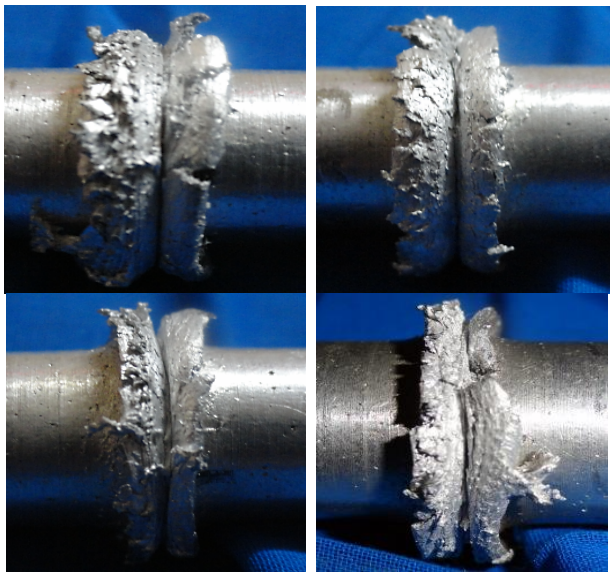

Fig. 4. Macro-view of friction welded joints.

3.1 Phase I: TOPSIS

Step 1: Establish the matrix A for multi attribute decision making (MADM) using the calculated S/N ratio values (η) for the responses. This was done as a part of data pre-processing [17, 18]. The S/N ratio was calculated for larger-the-better quality characteristic using Eq. (1).

$$A = \begin{bmatrix} \eta_1^1 & \cdots & \eta_n^1 \\ \cdots & \cdots & \cdots \\ \cdots & \cdots & \cdots \\ \cdots & \cdots & \cdots \\ \eta_1^m & \cdots & \eta_n^m \end{bmatrix}$$

where m = number of trials, η_i^j = performance of attributes from responses, $i = 1, 2\ldots n$ and $j = 1, 2\ldots m$.

Table 2. Calculated values of grey separation measure coefficient and GSMG.

Trial	S/N ratio			MADM matrix			Distance from ideal-negative solution			Grey separation measure coefficient			GSMG
	TS	WA_H	HAZ_H	TS	WA_H	HAZ_H	TS	WA_H	HAZ_H	TS	WA_H	HAZ_H	
1	39.46	37.26	36.77	0.335	0.328	0.327	0.108	0.188	0.146	0.204	0.318	0.302	0.275
2	39.15	37.95	37.61	0.333	0.334	0.334	0.060	0.391	0.383	0.195	0.383	0.375	0.318
3	39.33	36.52	35.84	0.334	0.321	0.319	0.086	0.051	0.014	0.200	0.285	0.273	0.252
4	38.91	38.06	37.72	0.331	0.335	0.335	0.032	0.429	0.423	0.191	0.399	0.391	0.327
5	38.43	37.38	36.90	0.327	0.329	0.328	0.002	0.218	0.174	0.186	0.326	0.309	0.274
6	38.23	39.55	38.98	0.325	0.348	0.347	0.000	1.147	1.010	0.186	1.638	1.028	0.951
7	39.11	38.58	38.38	0.332	0.339	0.341	0.055	0.643	0.696	0.194	0.515	0.549	0.419
8	41.33	35.70	35.41	0.351	0.314	0.315	0.693	0.000	0.000	0.427	0.274	0.270	0.324
9	38.44	39.55	39.18	0.327	0.348	0.348	0.003	1.147	1.122	0.186	1.638	1.493	1.106

$$S/N\ Ratio(\eta) = -10\log_{10}\left(\frac{1}{n}\right)\sum_{i=1}^{n}\frac{1}{y_{ij}^2} \tag{1}$$

where n = number of replications, k = number of observations, $i = 1,2,3\ldots n$ and $j = 1,2,3\ldots k$.

***Step 2*:** Calculate the normalized S/N ratio (x_i^j) using Eq. (2). This was done to avoid the effect of variability among the S/N ratio and for scaling the data [14]. The normalized S/N ratio varies as $0 \le x_i^j \le 1$.

$$x_i^j = \frac{\eta_i^j}{\sqrt{\sum_{j=1}^{m}\left(\eta_i^j\right)^2}}. \tag{2}$$

Step 3: Construct the normalized matrix A^N using the normalized S/N ratio values.

$$A^N = \begin{bmatrix} x_1^1 & . & . & . & x_n^1 \\ . & . & . & . & . \\ . & . & . & . & . \\ . & . & . & . & . \\ x_1^m & . & . & . & x_n^m \end{bmatrix}.$$

Step 4: Determine the distance of j^{th} alternative from the ideal-negative solution [17, 18] for each response using Eq. (3).

$$d_i^j = \left(x_i^j - x_i^-\right)^2 \text{ for } i = 1, 2\ldots, n \tag{3}$$

$$x_i^- = \min\{x_i^j, \text{for } j = 1,2,...,m\} \forall x_i^j (i = 1,...,n; j = 1,...,m;).$$

3.2 Phase II: Grey relational analysis

The maximization of distance of j^{th} alternative from ideal-negative solution would give the desired results. The process of grey relational generation [19] was employed to transform the distance of alternatives from ideal-negative solution into grey separation measure grade (GSMG).

Step 5: Compute the grey separation measure coefficient (γ) to express the relationship between best and actual distance of alternatives from negative-ideal solution using Eq. (4).

$$\gamma\left[d_0(k), d_i(k)\right] = \frac{\Delta\min + \xi\Delta\max}{\Delta_{oj}(k) + \xi\Delta\max} \tag{4}$$

where $\Delta_{oj}(k) = \left\|d_0(k) - d_i(k)\right\|$ was the absolute value of difference between $d_0(i)$ and $d_j(i)$, $d_0(i)$ was the reference sequence ($d_0(i) = 1;\ i = 1,2,\ldots,n$), dj(i) was the specific comparison sequence, $\Delta\min = \min\left\|d_0(k) - d_i(k)\right\|$ was the smallest value of $d_j(i)$, $\Delta\max = \max\left\|d_0(k) - d_i(k)\right\|$ was the largest value of $d_j(i)$ and ξ was the distinguishing coefficient whose value was taken as 0.33 to ensure equal importance for all the three responses during analysis.

Step 6: Calculate the GSMG values for each trial using Eq. (5).

$$GSMG_j = \frac{1}{n}\sum_{i=1}^{n}(\gamma_i). \tag{5}$$

The calculated values of S/N ratio, grey separation measure coefficient and GSMG are listed in Table 2.

Step 7: Determine the optimal level of welding parameters based on GSMG values. The main effect (ε_i) of the parameters was calculated using Eq. (6).

$$\varepsilon_i = \max(\overline{GSMG_{ij}}) - \min(\overline{GSMG_{ij}}). \tag{6}$$

Table 3. Main effects of the parameters on GSMG.

Parameters	Level 1	Level 2	Level 3	Max-Min
FP	0.2820	0.5175	**0.6167**	0.3347
UP	0.3407	0.3054	**0.7701**	0.4646
S	0.5167	**0.5839**	0.3157	0.2682
BOL	0.5518	**0.5630**	0.3014	0.2616

Table 4. Results of pooled ANOVA.

Source of variance	Sum of squares	Degrees of freedom	Mean sum of squares	F-ratio	% Contribution
FP	0.1773	2	0.0887	1.5176	21.44
UP	0.4015	2	0.2007	3.4363	48.55
BOL	0.1313	2	0.0656	1.1237	15.88
Error	0.1168	2	0.0584		14.13
Total	0.8269	8			100

The best level j^* of the controllable factor 'i' was selected as $j^* = max\ (GSMG_{ij})$. The main effects are summarised in Table 3 and the optimal levels of factors were identified as FP_3 UP_3 S_2 BOL_2.

Step 8: Calculate the predicted S/N ratio ($\bar{\eta}$) at the selected optimal level [19] of parameters from Eq. (7).

$$\bar{\eta} = \eta_m + \sum_{i=1}^{f} \left(\bar{\eta}_i - \eta_m \right). \tag{7}$$

η_m = Average S/N ratio, f = Number of control factors (parameters), $\bar{\eta}_i$ = Average S/N ratio corresponding to the i^{th} factor on the f^{th} level.

Step 9: Perform analysis of variance (ANOVA) to predict the contribution of significant factors in influencing the responses [20] and conduct the confirmation test for validation.

The results of pooled ANOVA are shown in Table 4. The parameter with the least contribution (rotational speed) was considered as error.

4. Results and discussion

Pores and shrinkage cavities were formed during the conventional liquid phase joining of Al/SiCp composites. The higher heat input combined with quicker cooling rate does not allow gases to escape out of it. The effect was more pronounced at higher viscosity of weld pool influenced by the reinforcement particles. During friction welding the temperature was kept significantly below the melting point of parent material. Further smaller welding time ensures reduced thermal stresses amid the matrix and reinforcement [8]. No alteration in the composition of the parent material was observed due to absence of fillers or electrodes.

The process involves three distinct phases: the initial phase, transition phase and forging phase. During the initial phase,

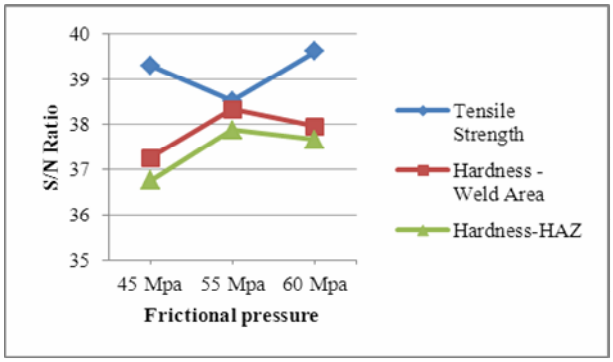

(a)

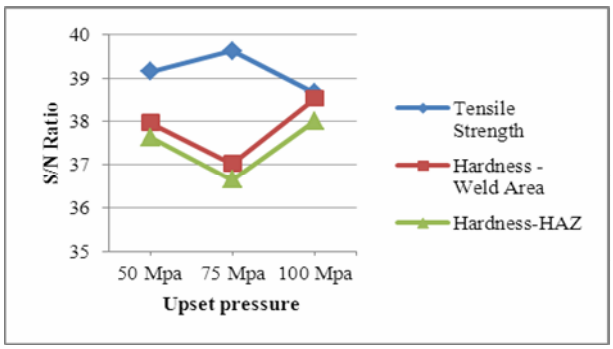

(b)

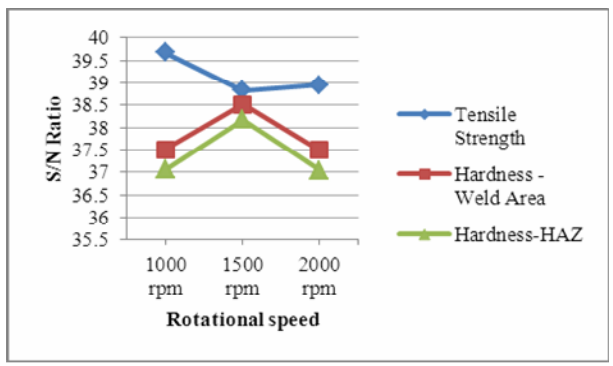

(c)

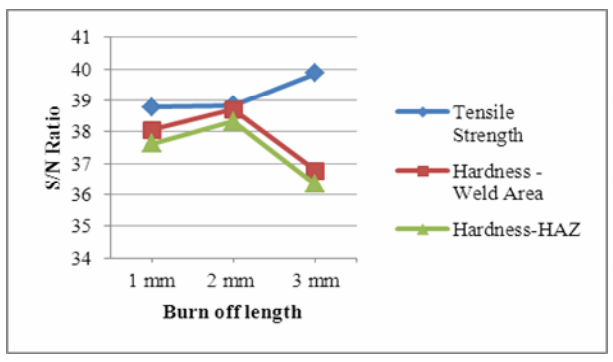

(d)

Fig. 5. Effect of parameters on the responses: (a) frictional pressure; (b) upset pressure; (c) rotational speed; (d) burn off length.

Table 5. Comparison between the responses obtained with the initial and the optimal parameter setting.

Responses	Initial parameter Setting		Optimal parameter setting using T-GRA		Improvement (%)	
	Observed S/N ratio	Response value	Predicted S/N ratio	Response value	S/N ratio	Response value
TS	38.441	83.57	41.502	86.31	0.061	1.74
WA_H	39.554	95	40.184	101	0.630	6.00
HAZ_H	39.181	91	39.889	98	0.709	7.00
Parameter settings	$FP_3\ UP_3\ S_2\ BOL_1$		$FP_3\ UP_3\ S_2\ BOL_2$			

thermal softening was observed at the interface due to applied mechanical rotation and frictional pressure. Surface asperities were worn out thereby increasing the contact area but no weld penetration was observed. True contact area was established due to plasticization of the interface during the transition phase. The heat lost due to conduction, forced convection and radiation was compensated by the combined effect of pressure and rotation. The HAZ was observed to spread from the asperities to the parent material but no axial shortening was detected. Finally during the forging phase, severe plastic deformation was observed at the interface and the material was expelled in the form of flash. This was characterized by axial shortening as well. It was observed that the deformation was largely circumscribed to the volume of material closer to the interface. The micro-hardness in the weld area was relatively higher than that observed in the HAZ due to oxidation during joining.

The effect of input parameters on the responses was studied by plotting the S/N ratio values for different levels of each parameter. It was observed that the tensile strength had improved at higher level of frictional pressure (60 MPa) but micro hardness was observed to be better at moderate value of frictional pressure (Fig. 5(a)). A moderate value of upset pressure (75 MPa) was found to produce joint with good tensile strength while higher value (100 MPa) was desired for better micro hardness (Fig. 5(b)). A lower value of speed (1000 rpm) was found to produce better tensile strength while moderate value (1500 rpm) was desired for good micro hardness values (Fig. 5(c)). Higher value of burn off length (3 mm) was observed to improve the tensile strength of joints (Fig. 5(d)).

The GSMG value was identified as the overall representative for all the three responses and the graphical plot of GSMG values for various trials is shown in Fig. 6. The maximum value of GSMG was observed for the trial number nine indicating the closeness of the parameter setting to the optimal welding condition.

It was observed that the contribution of upset pressure (48.55%) was more in influencing the responses followed by the frictional pressure (21.44%), while the other two parameters speed (14.13%) and burn off length (15.88%) were found to be less influential (Table 4). After obtaining the optimal level of input parameters using T-GRA methodology, confirmation test was conducted at the optimal combination of

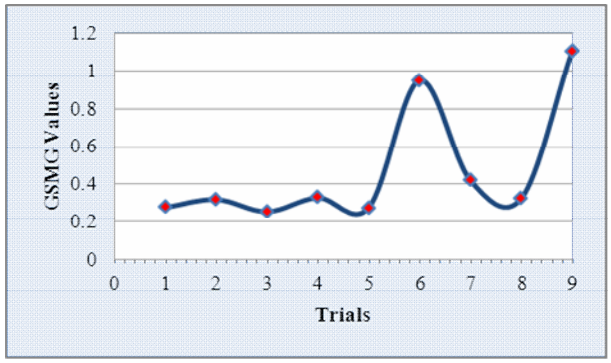

Fig. 6. Variation of GSMG values for various trials.

Fig. 7. Joint formed with optimal parameter setting (frictional pressure: 60 MPa, upset pressure: 100 MPa, burn off length: 2 mm and rotational speed: 1500 rpm).

$FP_3UP_3S_2BOL_2$. The joint formed with the optimal setting is shown in Fig. 7.

The plastic deformation of the material in the form of a symmetric flash (Fig. 7) was clearly evident in the optimal joint. The width of the flash was also found to be uniform on both sides of the bond line. The joint was subjected to tensile testing and the fractured surface was examined to study the failure mode. Generally a good degree of adhesion was found between the matrix and reinforcement (Fig. 8(b)). However due to external loading and consequence of particle debonding, small voids were seen (Fig. 8(a)). The size of the voids was reduced due to the plastic flow of surrounding material. The fractured surface was characterized by the presence of secondary cracks (Fig. 8(b)) and cracking of reinforcing

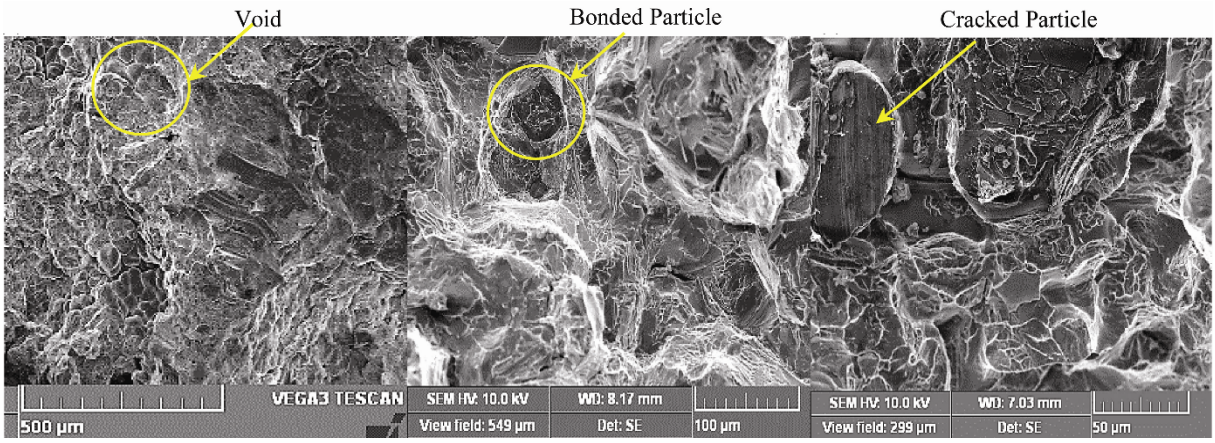

Fig. 8. FESEM images of the fractured surface.

particle (Fig. 8(c)) proving a predominantly ductile mode of failure.

The results of the confirmation experiment conducted at the optimal parameter setting were compared with those obtained with the initial parameter setting (Table 5). This confirmatory test gave satisfactory results and revealed the effectiveness of proposed method (T-GRA) in experimental welding optimization.

5. Conclusion and future scope

An integrated algorithm (T-GRA) was presented for optimizing the parameters in friction welding of Al6061/SiCp composites and the following conclusions were drawn:

(1) Severe plastic deformation and strain hardening were found to be the cause for increased micro hardness in the weld area relative to the HAZ.

(2) The integrated T-GRA algorithm was found to combine the ranking abilities of TOPSIS with the uncertainty handling capabilities of grey theory to predict the optimal setting of FW parameters.

(3) The optimal parameter combination predicted by the T-GRA approach (frictional pressure-60 MPa, upset pressure-100 MPa, burn off length-2 mm and rotational speed-1500 rpm) had significantly improved the S/N ratio and enhanced the quality characteristics observed in the process.

(4) Upset pressure was identified as the major controllable factor affecting multiple performance characteristics with a desired contribution of 48.55%, followed by the frictional pressure with a contribution of 21.44%.

(5) The FESEM images of fractured surface revealed small voids, secondary cracks in matrix and cracking of reinforcing particles proving a predominantly ductile mode of failure of these joints.

The research findings offer the required guidelines and database for welding Al6061/SiC_p composites using continuous drive friction welding process and the proposed algorithm (T-GRA) could be used for experimental welding optimization. However the interaction effects among parameters require further investigation. In future importance should also be given for the qualitative variables affecting the responses and studying the correlation between the quantitative and qualitative variables could be another contribution to the subject.

Acknowledgement

The authors would like to express their gratitude to Indian Institute of Technology Madras, for extending the facility to carry out the research work. Constant support from M. Santhanakumar, Assistant Professor, Department of Mechanical Engineering, Saveetha Engineering College, Chennai is highly appreciated.

References

[1] J. M. Torralba, C. E. Da Costa and F. Velasco, P/M aluminum matrix composites: an overview, *J. Mater. Proc. Technol.,* 133 (1) (2003) 203-206.

[2] M. B. D. Ellis, Joining of aluminium based metal matrix composites, *Int. Mater. Rev.,* 41 (2) (1996) 41-58.

[3] M. Maaklekian, Friction welding-Critical assessment of literature, *International journal of Science and Technology of Welding and Joining*, 12 (2007) 738-759.

[4] H. E. Akata and M. Sahin, An investigation on the effect of dimensional differences in friction welding of AISI 1040 specimens, *Industrial Lubrication and Tribology*, 55 (5) (2003) 223-232.

[5] M. Sahin, Joining of aluminium and copper materials with friction welding, *Int. J. Adv. Manuf. Technol.*, 49 (2010) 527-534.

[6] S. Hazman, I. M. D. Ahmad, R. Endri and A. A. Zainal, Mechanical evaluation and thermal modelling of friction welding of mild steel and aluminium, *J. Mater. Proc. Technol.*, 210 (10) (2010) 1209-1216.

[7] M. Selvaraj, Vela Murali and S. R. Koteswara Rao, Mechanism of Weld Formation during Friction Stir welding of Aluminum Alloy, *Materials and Manufacturing Processes*

DOI:10.1080/10426914.2013.763956 (in press, available online).

[8] F. Rotundo, L. Ceschini, A. Morri, T. S. Jun and A. M. Korsunsky, Mechanical and microstructural characterization of 2124Al/25 vol.%SiCp joints obtained by linear friction welding, *Composites: Part A*, 41 (2010) 1028-1037.

[9] K. Y. Benyounis and A. G. Olabi, Optimization of different welding processes using statistical and numerical approaches-A reference guide, *Advances in engineering software*, 39 (6) (2008) 483-496.

[10] R. Panneerselvam, *Design and analysis of experiments*, Prentice-Hall India, Eastern Economy Edition, New Delhi (2012).

[11] M. Madić and M. Radovanović, Application of RCGA-ANN approach for modeling kerf width and surface roughness in CO2 laser cutting of mild steel, *J. Braz. Soc. Mech. Sci. Eng.*, 35 (2) (2013) 103-110.

[12] S. P. Dwivedi, Sudhir Kumar and Ajay Kumar, Effect of turning parameters on surface roughness of A356/5% SiC composite produced by electromagnetic stir casting, *Journal of Mechanical Science and Technology*, 26 (12) (2012) 3973-3979.

[13] N. Muhammad, Y. H. P. Manurung, M. Hafidzi, S. K. Abas, G. Tham and E. Haruman, Optimization and modeling of spot welding parameters with simultaneous multiple response consideration using multi-objective Taguchi method and RSM, *Journal of Mechanical Science and Technology*, 26 (8) (2012) 2365-2370.

[14] R. Adalarasan, M. Santhanakumar and A. Shanmuga Sundaram, Optimization of weld characteristics of friction welded AA 6061- AA 6351 joints using grey-principal component analysis, *Journal of Mechanical Science and Technology*, 28 (1) (2014) 301-307.

[15] L. Singh, R. A. Khan and M. L. Aggarwal, Empirical modeling of shot peening parameters for welded austenitic stainless steel using grey relational analysis, *Journal of Mechanical Science and Technology*, 26 (6) (2012) 1731-1739.

[16] D. Yong, Plant location selection based on fuzzy TOPSIS, *Int. J. Adv. Manuf. Technol.*, 28 (7-8) (2006) 839-844.

[17] A. A. Mousa, Using genetic algorithm and TOPSIS technique for multi objective transportation problem: a hybrid approach, *Int. J. Comput. Math.*, 87 (13) (2010) 3017-3029.

[18] N. Ramkumar, P. Subramanian and M. Rajmohan, A multi-criteria decision making model for outsourcing inbound logistics of an automotive industry using the AHP and TOPSIS, *Int. J. Enterprise Netw Manag.*, 3 (3) (2009) 223-245.

[19] P. Narender singh, K. Raghukandan and B. C. Pai, Optimization by grey relational analysis of EDM parameters on machining Al-SiCp10% composites, *Journal of Materials Processing Technology*, 155-156 (2004) 1658-1661.

[20] R. Adalarasan, M. Santhanakumar, A. Shanmugasundaram and M. Rajmohan, Optimization of weld characteristics of friction welded Al/SiCp composites using grey relational analysis and principal component analysis, *Wulfenia Journal*, 20 (1) (2013) 422-433.

R. Adalarasan received his M.E. degree in Production Engineering from the Faculty of Engineering and Technology, Annamalai University in 2000 and currently works as an Associate Professor in the Department of Mechanical Engineering at Saveetha Engineering College, Chennai, India. He has authored more than 15 papers published in international journals and at international conferences. His research interests include welding processes, MMCs, optimization and meta-heuristics.

A. Shanmuga Sundaram is a citizen of India, born in Vellore, Vellore District, Tamilnadu on June 26, 1978. He received his Bachelor's degree in Mechanical Engineering with First Class in the year 1999 from the Bharathiar University Tamilnadu. He obtained his Master's degree with First Class in the field of Thermal Engineering from the University of Madras, Tamilnadu in the year 2000. He received his Ph.D. at Anna University, Chennai in 2009. He is currently working as Professor at Sree Sastha Institute of Engineering and Technology, Chennai-600123, India. His research interests are thermal management of electronics, thermal energy storage and heat transfer.